Side-by-side comparison of 3-C land streamer versus planted geophone data at the Priddis test site

Gabriela M. Suarez and Robert R. Stewart

ABSTRACT

A land streamer survey was successfully conducted by the CREWES Project in an area located in the foothills of the Canadian Rocky Mountains. The land streamer experiment was composed of two 3-C receiver lines located side-by-side: a land streamer and a planted geophone. Comparison of raw shot gathers, spectral analysis and stacked sections showed that the vertical channel data quality was found to be similar for both datasets, while the radial channel data was found to have highest quality for the planted geophone line. The signal bandwidth of the P-P reflections was fairly consistent along the receiver locations for the individual datasets, and correlated well between both experiments. For the P-S case there was no consistency within the land streamer dataset, nor any correlation with the conventional dataset.

INTRODUCTION

Over the past two decades, high-resolution seismic methods have become popular for resolving a wide variety of geological, engineering, and environmental problems (van ver Veen et al., 2001). Investigations such as these require the imaging of shallow targets (<300 m) using densely spaced sources and receivers, which are usually distributed over short acquisition spreads. However, using the traditional technique of planting geophones in the ground and physically moving cables in a CDP roll-along is costly, labour and time-consuming, especially for shear-wave surveys with their requirement for smaller spatial sampling (Pugin et al., 2004). To address some of these issues, towed land-streamer systems have been in use since the 1970s.

A land streamer could be defined as an array of geophones designed to be towed along the ground without planting. This idea comes from the seismic marine industry, where large volumes of high-resolution data are recorded using marine streamers. However, the first tests on land were restricted to ice or snow (snow streamer), both of which provide smooth sliding surfaces suitable for long streamer use and a good geophone coupling (van ver Veen et al., 2001). The concept of a towed land cable was patented by Kruppenbach and Bedenbender (1975; ibid, 1976).

Numerous successful case studies have been presented during the last three decades, helping to improve the near-surface imaging (van der Veen et al., 1998; ibid,1999; ibid, 2001; Pugin et al., 2004; Ivanov et al., 2006; Lorenzo et al., 2006; Inazaki, 2006; Speece et al., 2007). To further develop this technology, especially for converted-wave recording, the CREWES Project acquired a 3-C land-streamer system. The first experiment was conducted during summer 2007 in the Priddis area located southwest of Calgary, Alberta. The objective of this first attempt was to image the upper 50 m of the subsurface, test the capabilities of this acquisition technique, and proposed future improvements that need to be undertaken to achieve better quality seismic data (Suarez and Stewart, 2007). A second test was conducted in the same location during March 2008

but with the objective of doing a side-by-side comparison of a planted 3-C geophone line and a land streamer line. This paper describes the second experiment and discusses the results of the comparison from both acquisition systems.

Location

The survey area was located about 5 km from the town of Priddis in the foothills of the Canadian Rocky Mountains, southern Alberta (Figure 1). Our geophysical test site is also home to the University of Calgary's Rothney Astrophysical Observatory. This area has been a location of extensive shallow VSP experiments by the CREWES project (Wong et al., 2007) and a 3D seismic survey (Lawton et al., 2008).
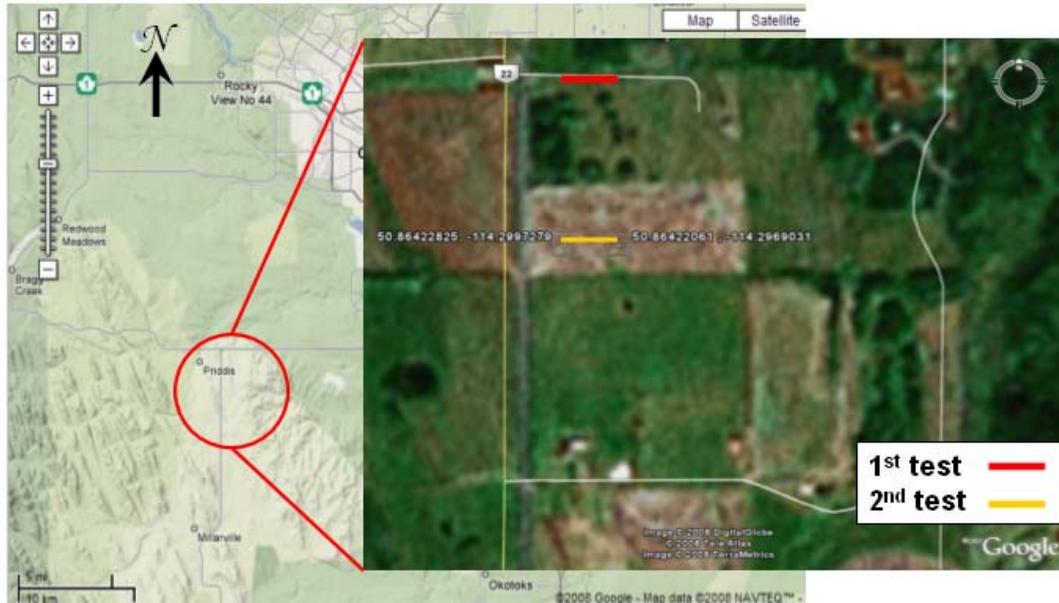

FIG. 1. Aerial photograph showing the location of the study area: The first test on dirt road (red line), the second test on grass covered hill (yellow line). Photograph from Google Earth.

Description of the survey

A side-by-side multicomponent seismic line configuration oriented nearly East-West was used for the test. The test consisted of a 200 m planted-geophone seismic line, a 20 m land streamer system and a 400 m source line (Figure 2). For the 2D "conventional line" we used 200 3-C geophones at a 1 m spacing. A land streamer configuration (1 m; 60 channels, 20 m total) was used over the grass-covered surface, with a 10 times cable roll with no overlapping, to reach the 200 m length of the comparison line.

The multicomponent survey employed a vibroseis source and multicomponent geophones. The source was an IVI Envirovibe (18,000 lb) sweeping from 10 to 250 Hz sweep with an 11 seconds listening time and a 4 times vertical stack. The receivers were 10 Hz 3-C geophones that were being recorded at a 1 ms sampling rate. The land streamer receivers were recorded by a Geometrics Geode recording system with 60 channels and the planted geophones or "conventional line" was recorded by an ARAM recording system. The 400 m total line length was acquired in 10 parts, where every part corresponds to a different location of the 20 m length land streamer. For every streamer

segment the 40 source locations spaced at 10 m were repeated, which means that the planted geophone line was recorded 10 times and the source line was fired 10 times. The first and last source points have a maximum offset of 300 m that correspond to the longest offset of the whole line. These two points were located 100 m off the receiver line. This maximum offset was being reduced 10 m with every location of the source until reaching the shortest offset of 200 m. This position corresponds to the location when the source is in the middle of the receiver line.

In total, 40 shot locations were acquired, 200 receiver stations, 10 land streamer positions and a total line length of 400 m for the source line and 200 m for the receiver line.
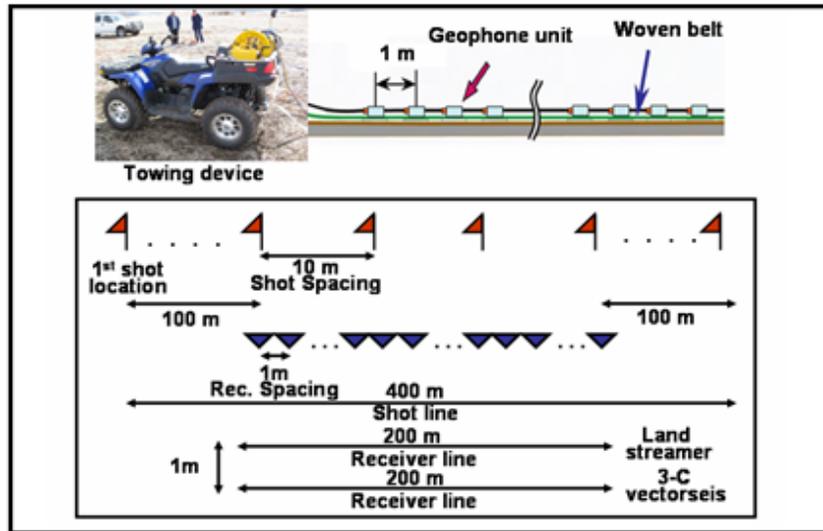

FIG. 2. Illustration of the land streamer configuration used on second (bottom) land streamer seismic experiment: a 20 m streamer with 3-C geophones separated 1 m, with a sledge hammer P-wave source located at 1 m off the cable (test 1) and a vibroseis source (test 2) (modified after Inazaki, 2006).

Processing

After acquisition, the coincident data sets were passed through the same processing sequence using identical processing parameters. The survey geometry resulted in a maximum fold of 19 for the vertical and for the radial channel sections.

The crucial step during the processing was the re-arrangement of the datasets to make them equivalent. Because the land streamer data was acquired using 10 runs of the same source line, the different segments have to be put together, numbered and sorted. Subsequently, a geometry was assigned to it to construct a 200 m seismic line. For the conventional line, the same process had to be done because of the 10 times that the same line was acquired. For every run the equivalent traces to the land streamer were chosen, the same receiver locations were killed, and the same numbering, sorting and geometry was assign to it.

ANALYSIS OF THE DATA

1) Comparison of shot gathers and stacked sections

1.1) Raw shot gathers:

In Figure 3, the responses of the various geophones of the vertical and radial channels for a raw shot gather are compared.

Vertical channel: Unprocessed source gathers recorded with the streamer and the conventional line are similar (Figure 3). The signal-to-ambient noise level is higher for the planted geophone line. On the raw shots for both datasets it is difficult to observe reflections as a consequence of the prominent coherent noise along the line, but differences are observed in the signal characteristics of the airwaves. They are strongest in the conventional data and weakest in the streamer data, probably because the latter suppress slightly the higher frequency signals (van ver Veen et al., 2001).

Radial channel: The unprocessed source gathers in the land streamer look noisier and the events do not look very coherent as in the conventional dataset (Figure 3c and 3d). The quality of the first breaks is poor for the land streamer. In general the source gather of the planted geophones shows much better signal, more coherency and less random noise.
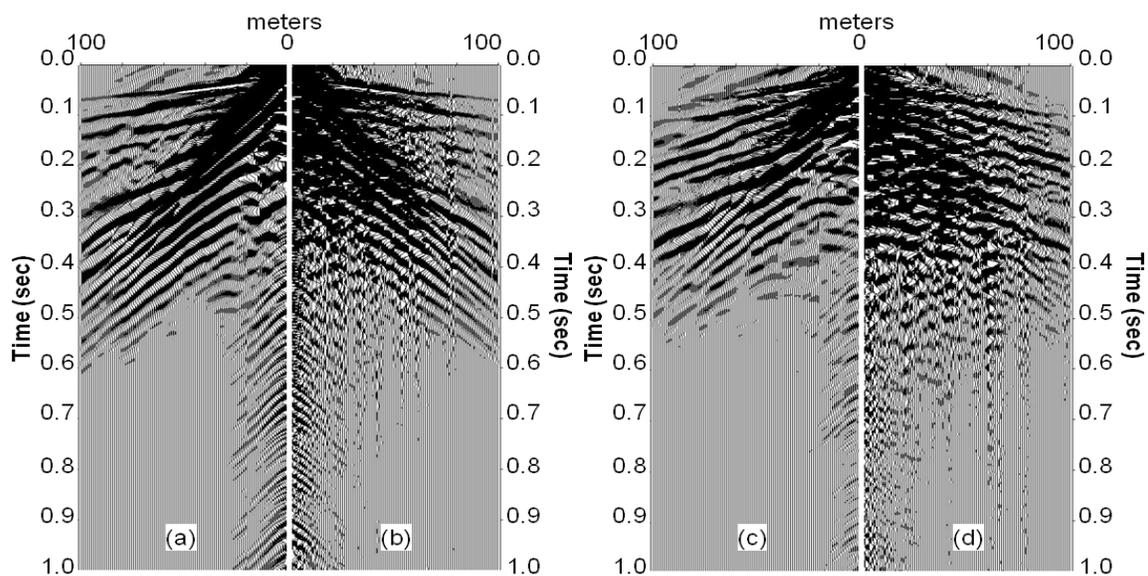

FIG. 3. Comparison of two raw shot gathers. In (a), half of a split spread record from the vertical component conventional line. The same shotpoint from the vertical component land streamer is shown on (b) with the lateral coordinate reverse to ease the comparison. The same comparison is done for the same record for the radial component of (c) the conventional line and of (d) the land streamer line.

1.2) Unmigrated stacked sections

Vertical channel: The few reflections existent in this area are reasonably well imaged on both stacked sections (Figure 4); however, the land streamer section looks more

contaminated with noise. There is a considerable difference in amplitude between the sections but the same events between 75 and 300 ms can be observed.

Radial channel: In the stacked sections for the radial channel the main reflections are present but they are not continuous throughout the line for the land streamer dataset (Figure 5). There are considerable differences in amplitude, events and signal-to-noise ratio for these two sections, where the quality of the streamer dataset is of much lower quality than for the vertical channel case, especially after 1.5 seconds where most of the reflectors that can be observed in the conventional lines cannot be observed on the land streamer. In both sections, there is still present a strong linear noise that could not be eliminated from the data during the processing, this noise trend is more prominent in the streamer data.
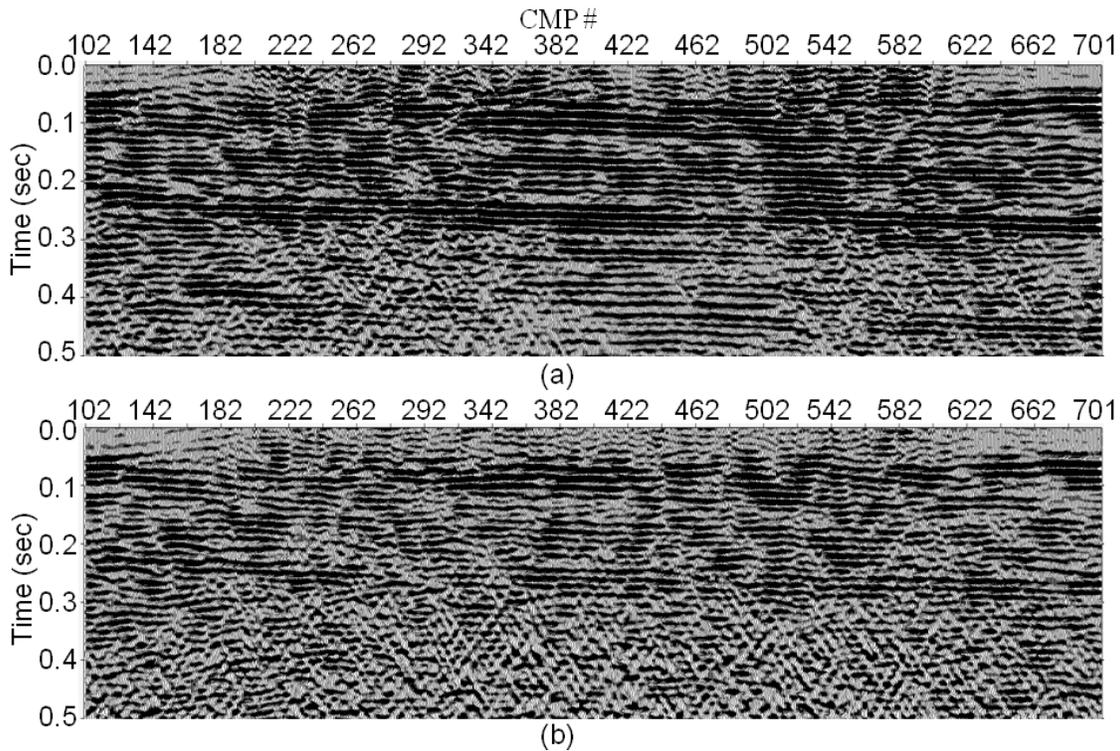

FIG. 4. Comparison of stacked sections in the vertical channel for the conventional line data (top) and for the land streamer data (bottom). Zoom of the first 0.5 seconds.
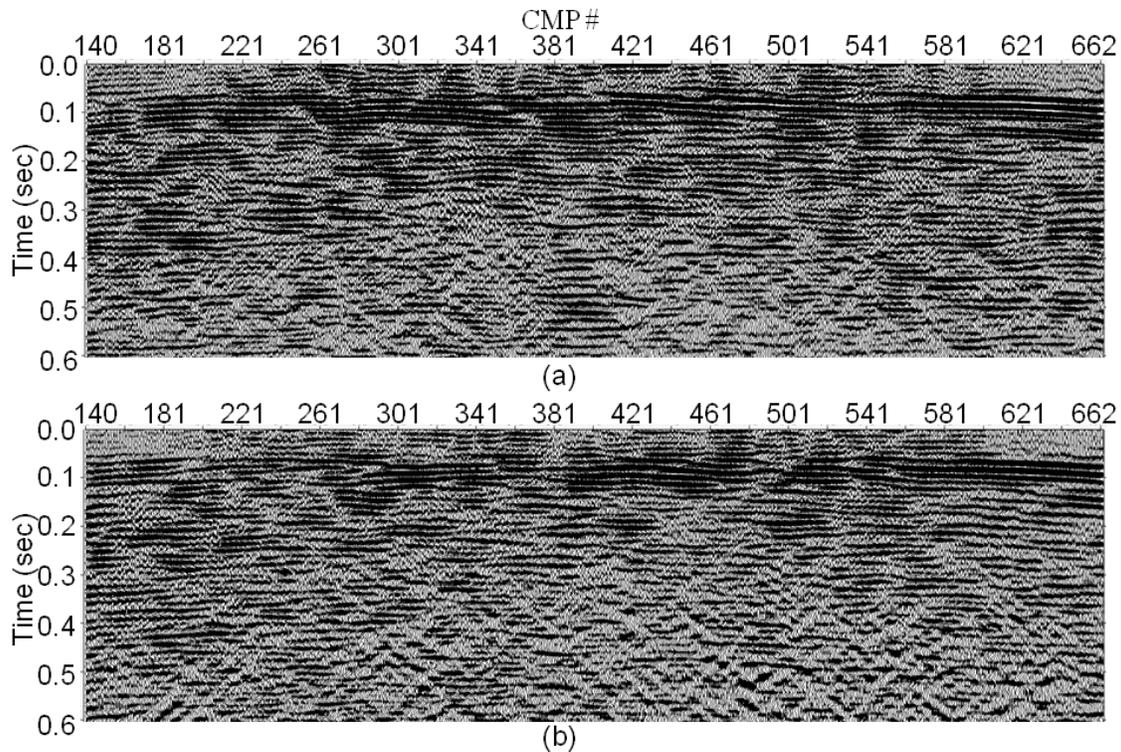
FIG. 5. Comparison of stacked sections in the radial channel for the conventional line data (top) and for the land streamer data (bottom). Zoom of the first 0.6 seconds.

2) Spectral analysis

2.1) F-x analysis of the raw shot gathers:

Vertical channel: An average Fourier amplitude spectrum was calculated on a raw shot gather for a window corresponding to a signal only area (Figure 6a). With this analysis is seen how the source gathers recorded with both systems are very similar: peaks and troughs match reasonably well up to 110 Hz. Both curves are similar up to 50 Hz, after which the land streamer shows greater power. It is important to mention that this comparison is not as diagnostic as with stacked data.

Using the same amplitude spectrum plot of Figure 6(a) and based on the potential band estimation method presented in Margrave (1999), we are trying to identify a "corner frequency" where the signal spectrum will drop below the background noise level. This observation will be corroborated on the f-x analysis of the unmigrated stacked sections. The corner frequency for these datasets is not as evident as in the examples presented in Margrave (1999); however, the spectrum shows a trough for both datasets at 160 Hz for the conventional line and at 180 Hz for the land streamer that might be the corner frequency, after this trough the decay rate gets similar for the remaining frequencies up to 250 Hz (maximum sweep frequency).

The same analysis was done in windows that cover a portion of the first breaks and noise (Figure 6b and 6c). These last analyses were done to see if both systems could record the same seismic events (signal and noise) with the same characteristics. For the

first break window (Figure 6b), both spectra are smooth and with similar shape, with the difference that the refractions show slightly greater energy for the land streamer.

For the window located in the noise area the results are very similar (Figure 6c), presenting the land streamer curve more peaks and troughs than the one for the conventional line after the first 80 Hz. In the range 0 to 80 Hz, the curves are very similar. For both datasets, the Rayleigh waves exhibit dominant frequency near 50 Hz, which is a very high dominant frequency for waves that usually have a much lower dominant frequency (around 8 Hz).

Radial channel: The same Fourier analyses were done in the radial channel (Figure 6). Surprisingly, in the signal only window peaks and troughs match reasonably well up to 140 Hz.

The result of the analysis on the first breaks window shows that both spectra have similar shape (Figure 6b). However, the curve corresponding to the conventional line shows more discontinuities along the frequency range. If we go back to the raw shot gathers (Figure 3c and 3d) we can notice how the first breaks for the land streamer present a better character than for the conventional line, not being so contaminated by the source generated noise in the near offsets.

For the window located in the noise area, the Rayleigh waves exhibit a dominant frequency of 30 Hz. From the raw gathers (Figure 6c) we saw how the noise was stronger on the land streamer than in the conventional line, this is corroborated in this spectrum where the amplitudes of the Rayleigh waves are higher for the land streamer.
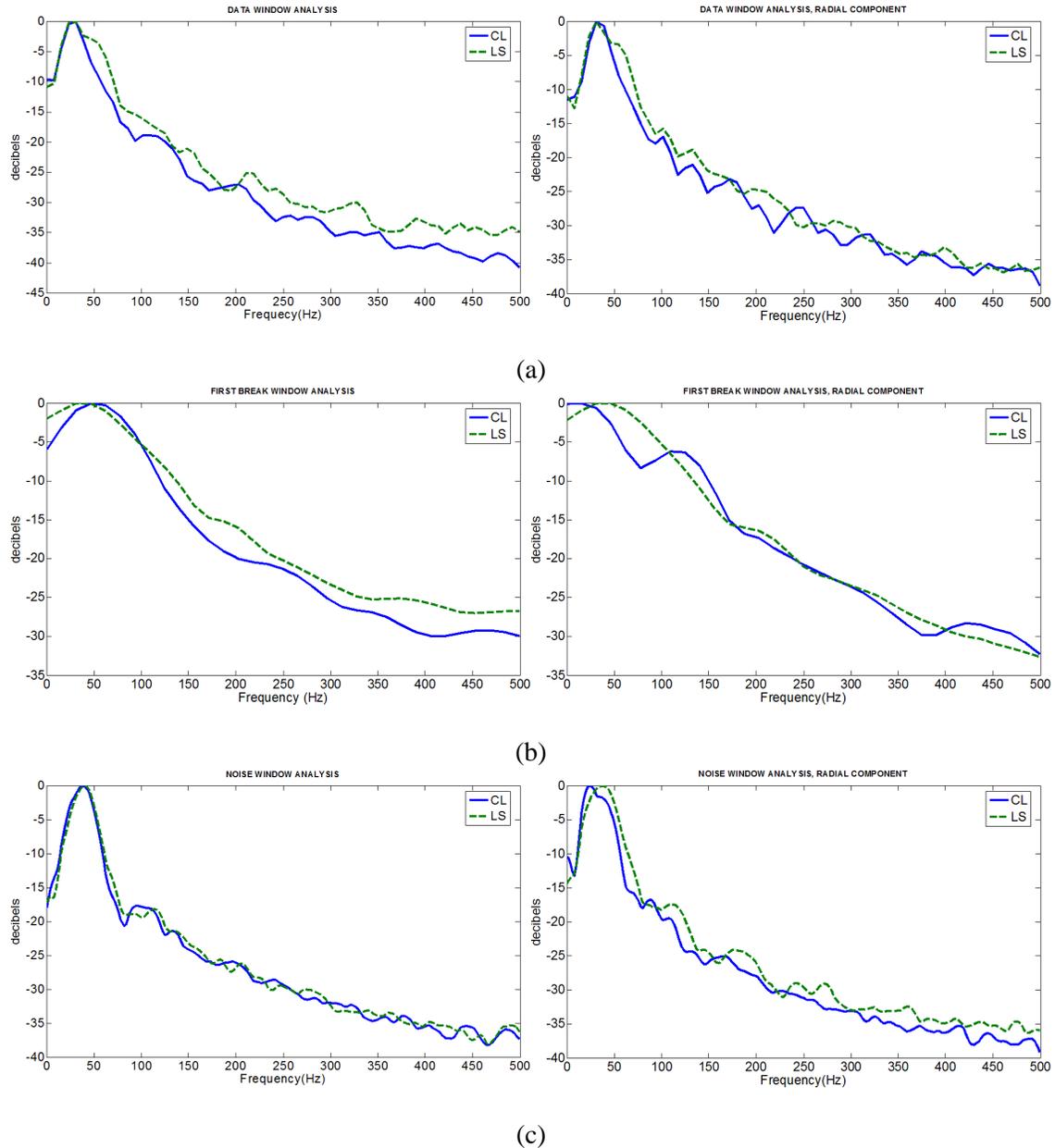
FIG. 6. Average Fourier amplitude spectrum of a raw shot gather for the vertical channel (left) and radial channel (right)of the conventional (CL) and land streamer line (LS), with windows corresponding to: (a) signal only area, (b) first break area and (c) groundroll/noise area.

2.2) F-x analysis of the unmigrated stacked sections

<u>Vertical channel</u>*:* An f-x analysis of both unmigrated, unfiltered stacked sections is shown in Figure 7 to estimate the realized signal band. The realized signal band method computes the f-x Fourier spectra of unmigrated stacked sections, and plots the amplitude and phase spectra separately. The frequencies where signal is dominant are recognized by laterally-coherent spectral events while spectral power is indicated by strong (dark) regions on the amplitude spectrum (Margrave, 1999; Hamarbitan and Margrave, 2001).

The f-x amplitude spectrum for both datasets (Figure 7a and 7b) shows a drop in spectral power above 160 Hz. The conventional line spectrum shows a drop above 110 Hz for CMP's 100 to 200 and 600 -700 that corresponds with the edges of the line.

The phase coherence of the two datasets is contrasted in Figure 7(c) and (d). For both datasets there is a sudden reduction in phase coherence at about 110 Hz coincident with the drop in spectral power in Figure 6(a) and (b). However, for the conventional line data subtle phase coherence persists up to 140 Hz, indicating low signal levels. In contrast, the land streamer show good phase coherence to about 90 Hz but very little at higher frequencies. These observations may be interpreted as indicating similar signal levels in the two datasets below 90 Hz. In the 90-140 Hz band, the strength of the conventional line is greater than that of the land streamer data. On the other hand, from 180 to 240 Hz, the land streamer data show evidence of weak signal towards the edges of the line, whereas the conventional line dataset shows coherent, weak signal along all the line.

<u>Radial channel</u>: The f-x amplitude spectra for both datasets for the radial channel are contrasted in Figure 8. Surprisingly, the phase and spectral power spectrum for the radial channel are very similar to the vertical channel (Figure 8), they show a drop in spectral power above 160 Hz. The conventional line spectrum does not show the drop in spectral power in the CMP range 100 to 200 at the ends of the line. The spectral power looks slightly weaker for the radial channel than for the vertical.

The land streamer spectrum is very similar than the conventional line, but it looks noisier for the very low and high frequencies.

The phase coherence of the two datasets is contrasted in Figure 8(c) and (d). For both datasets there is a sudden reduction in phase coherence at about 110 Hz coincident with the drop in spectral power in Figure 6(a) and (b). This observation coincides with the vertical channel, but in 40-110 Hz band of the radial channel the events look weaker. After 110 Hz, there are not strong events with good coherency. From 180 to 240 Hz, both datasets show evidence of weak signal.

The phase coherence plots are very similar for both lines; maybe a subtle difference is in the low frequencies where the conventional line appears to have a higher content of low frequencies.
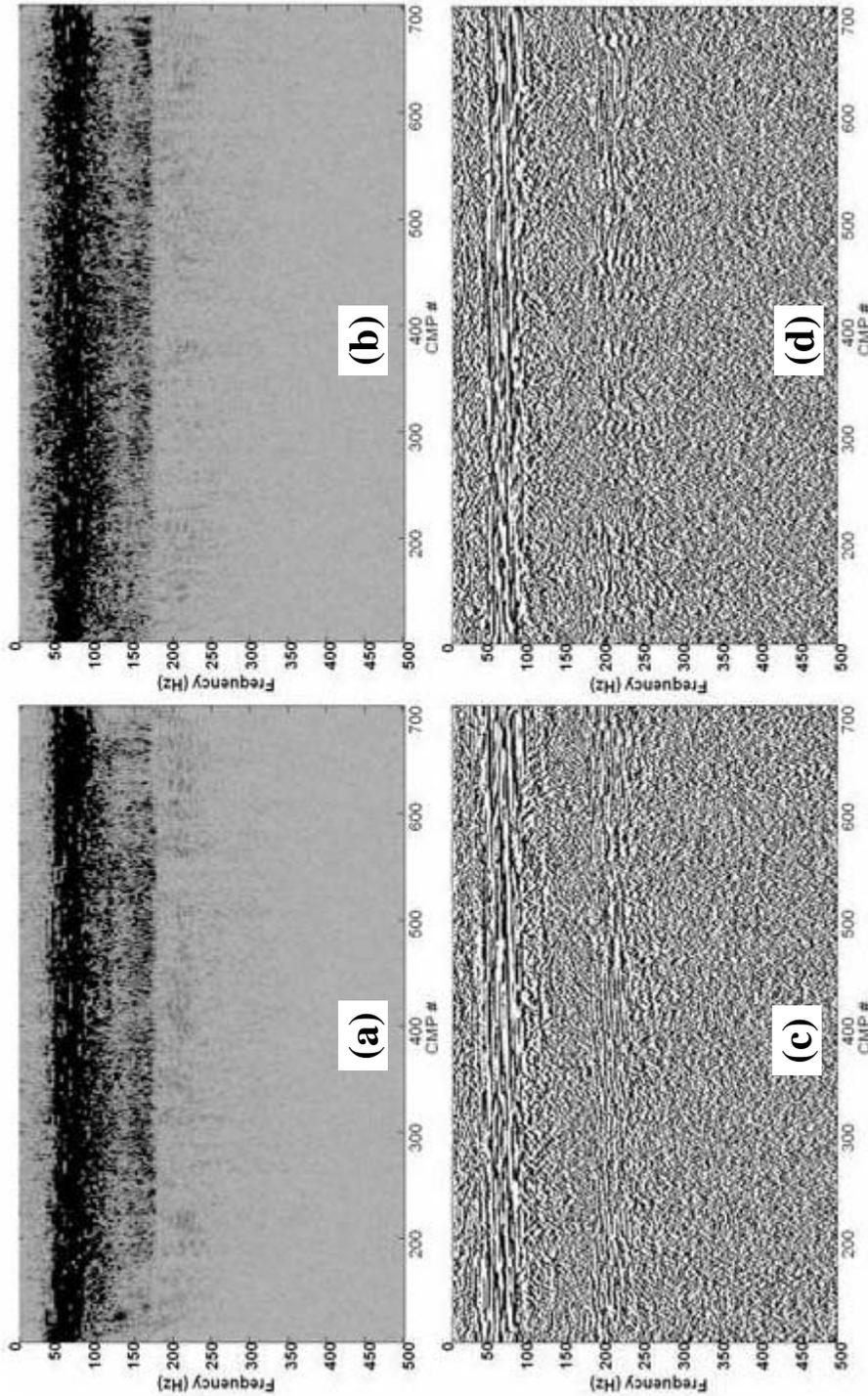
FIG. 7. F-x spectral analysis for the final unmigrated, unfiltered P-wave stack for the conventional line data and for the land streamer data computed over the time zone 70-300 ms. The f-x amplitude spectrum for the conventional line is shown in (a); (b) shows a similar spectrum for the land streamer data. The land streamer data shows reduced signal power above 80 Hz. In (c) and (d) the f-x phase spectra are shown corresponding to (a) and (b), respectively. The conventional line data show very low phase coherence from 100 to 180 Hz and very weak coherence from 180 to 240 Hz. The land streamer data show good phase coherence from 50 to 80 Hz and very little at higher frequencies.
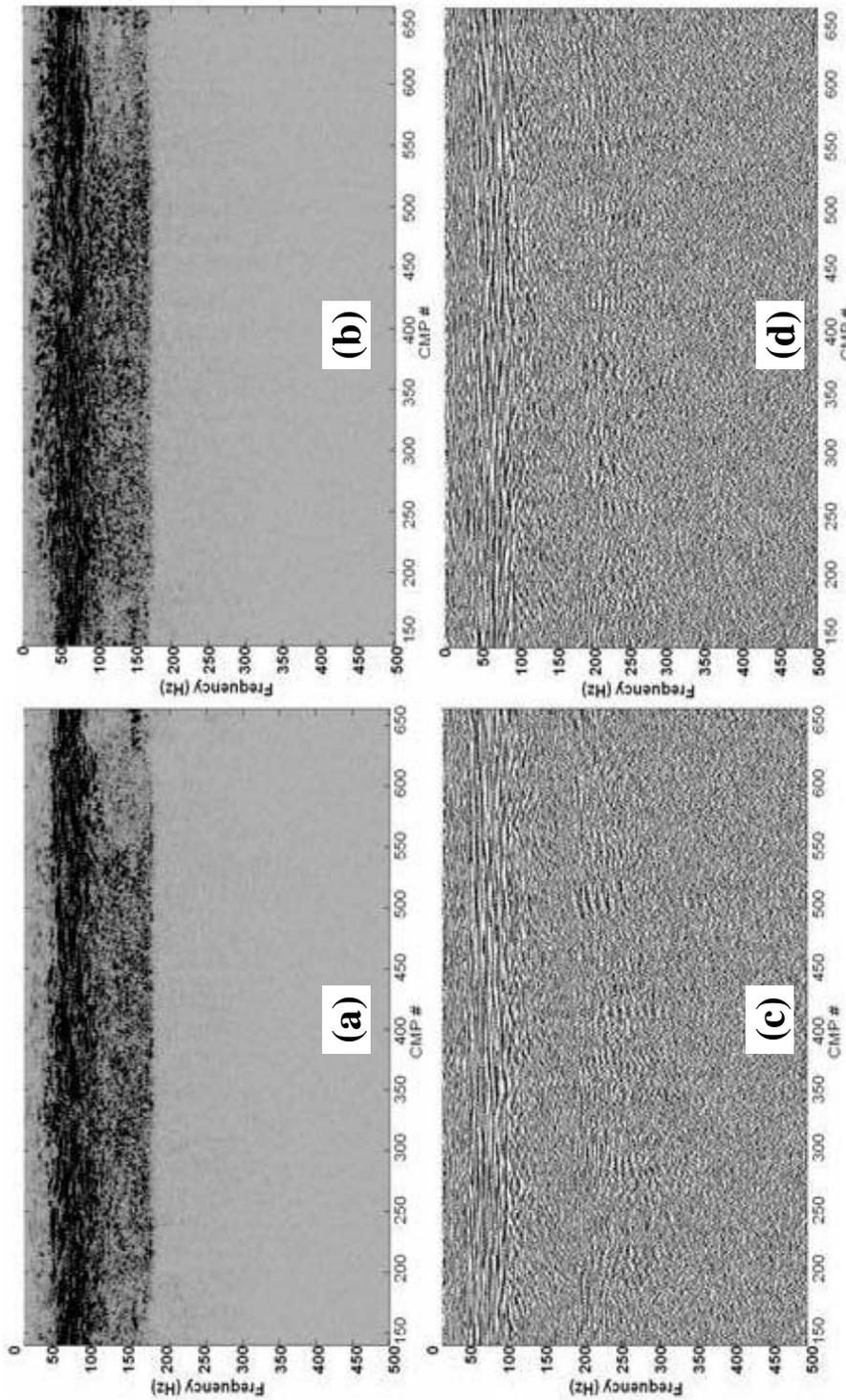
FIG. 8. F-x spectral analysis for the final unmigrated, unfiltered PS-wave stack for the conventional line data and for the land streamer data computed over the time zone 60-500 ms. The f-x amplitude spectrum for the conventional line is shown in (a); (b) shows a similar spectrum for the land streamer data. The land streamer data shows reduced signal power above 100 Hz. In (c) and (d) the f-x phase spectra are shown corresponding to (a) and (b), respectively. The conventional line data show very low phase coherence from 100 to 180 Hz and very weak coherence from 180 to 300 Hz. The land streamer data show good phase coherence from 50 to 100 Hz and very weak from 200 to 240 Hz. at higher frequencies.

3) Frequency Analysis of the receiver gathers

Signal bandwidth may depend on receiver location (i.e. its location along the receiver line) and receiver depth. However, geophone coupling and the quality of the geophone planting might be a controlling factor in the variation of the signal bandwidth as well, variation in bandwidth across the receiver line are considered to indicate variations in geophone coupling (Cieslewicz and Lawton, 1998).

The relationship between frequency content, receiver location and geophone coupling can be depicted by plotting the spectra data in three dimensions with contour plotting. For every receiver gather of every dataset, a separate frequency spectrum was calculated in the appropriate time window, creating a matrix that represent location along the receiver line; the rows represent frequencies from zero to nyquist; and each individual cell contains decibels below maximum amplitude of the frequency spectra.

Vertical channel: Figure 9(a) and (b) shows the frequency contour plots of the vertical channel for the conventional line and land streamer data. Between geophones of the two acquisition systems, the frequency spectra has a reasonably correlation between frequencies in the range 40-80 Hz. For low frequencies, amplitude attenuation is less for the land streamer than for the conventional line. For high frequencies, attenuation is higher for the streamer than for the planted dataset.

In the data, 70 Hz contamination can be seen, this should be consistent between all the receiver stations, but in the plot the consistency is better for the land streamer than for the other dataset where is only noticed at some segments of the line. This evidence is another indication of better receiver coupling for the land streamer in this frequency range.

Radial channel: Figure 9(c) and (d) show contoured plots of the difference in frequency spectra of converted-wave reflections for both datasets as recorded on the radial channel. For the radial channel there is a poor correlation between the frequency spectra of both datasets. The planted geophones do not have as great a variation in bandwidth across the receiver line as the land streamer phones. These observations indicate that for the converted-wave the geophone coupling was better for the planted geophone line.
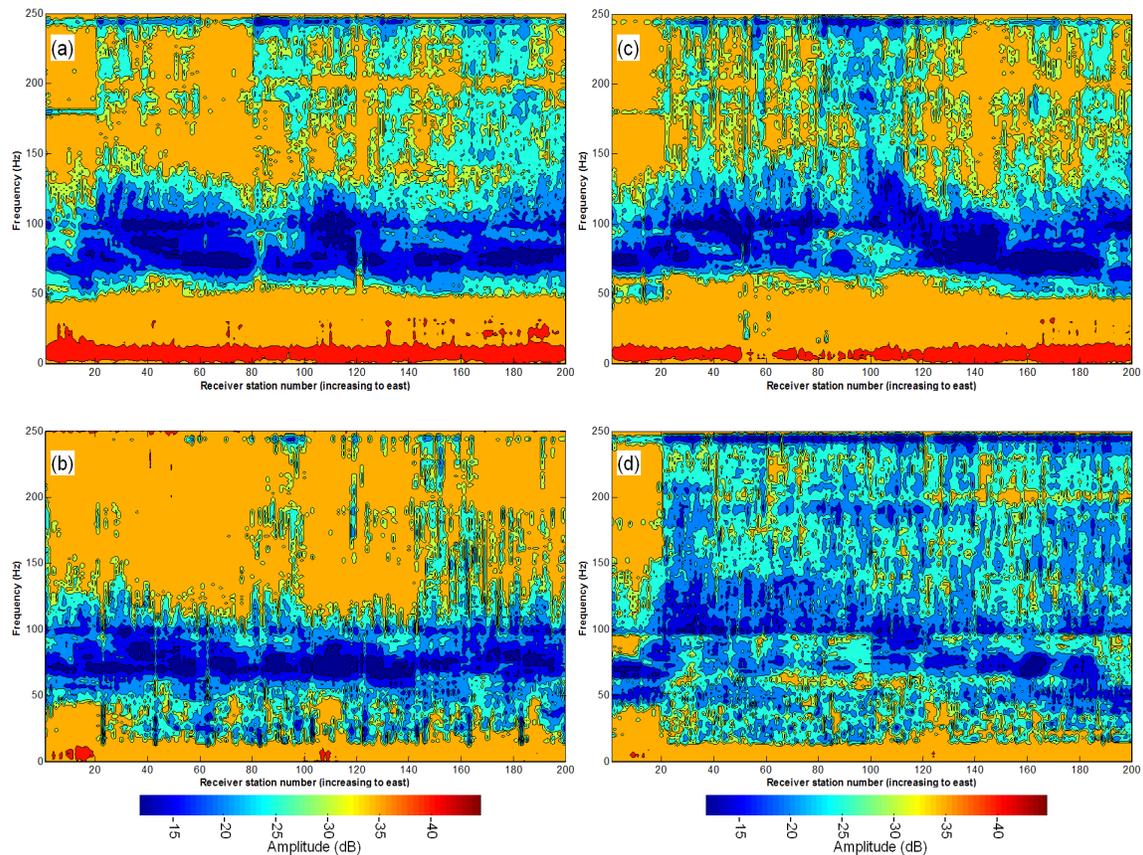
FIG. 9. Frequency Analysis of the common receiver gathers for both lines. In (a) and (b) is shown the resulted contour plot of the vertical channel conventional line and land streamer, respectively. In (c) and (d) is shown the same analysis but for the radial channel of the conventional line and land streamer data, respectively.

CONCLUSIONS

A comparison between a 3-C land streamer and a 3-C planted-geophone line was undertaken. The analysis indicates that for the vertical component the datasets show similar events and characteristics.

The land streamer system recorded high-resolution seismic data on a grass covered hill. Its geophone-to-ground coupling was good and very close to be matched with the planted geophone line for the vertical channel but not for the radial and transverse channels.

Employing a vibratory source improved the acquisition speed and offered the possibility of generating repeatable signals that were necessary to complete our experiment.

The raw shot gathers for the vertical channel were alike, showing the same characteristics for the noise, the first breaks and the reflections. For the radial and transverse channel the results suggested that even when the main reflections are shown, they are not very similar to the data from the planted geophones.

After identical processing, the processed stacked sections showed the existence of seismic reflections in the area and corroborated the same results as the raw shot gathers for the vertical and radial channels. An f-x spectral analysis of the stacked sections reveals that for the vertical channel both datasets signal levels are similar below 90 Hz, with a drop in spectral power above 160 Hz and a reduction in phase coherence at 110 Hz. The planted geophone dataset shows low signal levels up to 140 Hz. In the radial channel the observations about the phase and spectral power are very similar to the vertical channel. The land streamer spectra are similar to the conventional line, but with higher noise levels for the very low and high frequencies.

These results corroborate the benefits and versatility of this system when is compared with the conventional way we use to acquire seismic data. It shows its potential in reducing acquisition time and labour for land seismic operations. It also shows how good quality data can be generated in different environments, and its future as an exploration tool for oil, gas, environmental, engineering, archaeological and mining applications.

REFERENCES

Cieslewicz D. and Lawton D. C., 1998, The Blackfoot III buried geophone experiment: CREWES Research Report, **10**.

Hamarbitan, N.S. and Margrave, G.F., 2001, Spectral analysis of a ghost: Geophysics, **66**, 1267-1273.

Inazaki, T., 2006, High-resolution S-wave reflection survey in urban areas using a woven belt type land streamer : Near Surface 2006 Expanded Abstracts, Paper A016.

Ivanov J., Miller, R. D., Lacombe, P., Johnson, C. D. and Lane Jr., J. R., 2006, Delineating a shallow fault zone and dipping bedrock strata using multichannel analysis of surface waves with a land streamer: Geophysics, **71**, A39-A42.

Kruppenbach, J. A., and Bedenbender, J. W., 1975, Towed land cable: U. S. Patent 3 923 121. 1976, Towed land cable: U. S. Patent 3 954 154.

Lawton, D.C., Stewart, R.R., and Bertram, M.B., 2008, 3D seismic surveys for shallow targets: 2008 CSPG CSEG CWLS Convention abstract, 283-286.

Lawton, D.C., Stewart, R.R., and Bertram, M.B., 2008, 3D seismic surveys for mapping shallow targets: 2008 SAGEEP annual conference abstract, 8 p.

Lorenzo J. M., Saanumi, A., Westbrook, C., Egnew, S., Bentley, S. and Vera, E. E., 2006, Extensive testing of sled-mounted geophone arrays for near-surface (0-4m) layers in floodplain sedimentary facies: Atchafalaya Basin, Indian Bayou, Louisiana : 76th Ann. Internat. Mtg., Soc. Expl. Geophys., Expanded Abstracts, 1496-1499.

Margrave, G.F., 1999, Seismic signal band estimation using f-x spectra: Geophysics, **64**, 251-260.

Pugin, A. J. M., Larson, T. H., Sargent, S. L., McBride, J. H. and Bexfield, C. E., 2004, Near-surface mapping using SH-wave and P-wave land-streamer data acquisition in Illinois, U. S.: The Leading Edge, **23**, 677–682.

Speece M. A., Betterly, S. J., Levy, R. H., Harwood, D. M. and Pekar, S. F., 2007, An over-sea-ice seismic reflection survey in Antarctica using a GI air gun and a snowstreamer: 77th Ann. Internat. Mtg.,Soc. Expl. Geophys., Expanded Abstracts, 1-5.

Suarez, G. M. and Stewart R. R., 2007, Acquisition and analysis of 3C land streamer data: CREWES Research Report, **19**.

Telford, W.M., Geldart, L.P., and Sheriff, R.E., 1990, Applied Geophysics, Second Edition: Cambridge University Press.

van der Veen, M. and Green, A. G., 1998, Land-streamer for shallow seismic data acquisition: Evaluation of gimbal mounted geophones: Geophysics, **63**, 1408–1423.

van der Veen, M., Spitzer, R., Green, A. G. and Wild, P., 1999, Design characteristics of a seismic land streamer for shallow data acquisition, 61th EAGE Conference & Exhibition, Expanded Abstracts.

van der Veen, M., Spitzer, R., Green, A. G. and Wild, P., 2001, Design and application of a towed land-streamer system for cost-effective 2-D and pseudo-3-D shallow seismic data acquisition: Geophysics, **66**, 482–500.

Wong J., Miong S., Gallant E. V., Bland H. C., Bentley L. R. and Stewart R. R., 2007, VSP and well logs from the U of C test well : CREWES Research Report, **19**.